



VNIVERSITAT ID VALÈNCIA

First results of the CAL/VAL activities for Landsat 9 TIRS-2 at the Valencia test site

Raquel Niclòs, Martín Perelló, Jesús Puchades,
César Coll, Enric Valor

Thermal Remote Sensing Group, Department of Earth Physics and Thermodynamics
Faculty of Physics, University of Valencia

Introduction

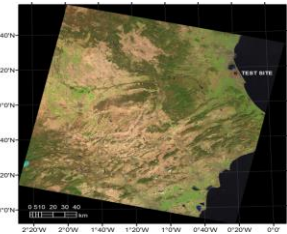
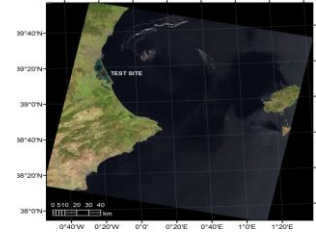
- Landsat 9 TIRS-2 instrument consists of two thermal infrared (TIR) bands, Band 10 and Band 11, which provide thermal TIR data with a spatial resolution of 100 meters (resampled to 30m) and a revisit time of 16 days.
- Evaluation of Landsat 9 TIRS-2 calibration in terms of brightness temperature and land surface temperature (LST) for very different ground covers and atmospheric conditions through December 2021 to January 2023 in the Valencia test site.
- Ground LST measurements, used as reference data, acquired along transects by multiband TIR radiometers over a thermally homogeneous site with different land covers due to phenology.
- Evaluation of a single-channel (SC) and split-window (SW) methods for atmospheric and emissivity corrections of L9 TIRS-2 brightness temperatures for LST retrievals.



Valencia test site

- Uniform and thermally-homogeneous rice paddy area near the city of Valencia.
- Previously used in CAL/VAL studies for other satellite sensors (Coll et al., 2005, 2012; Niclòs et al., 2018, 2021).
- Three different land covers at the site: full vegetation cover (July-September), bare soil (February-April), and flooded soil (December-January & May-June).
- Covered by L9 scenes acquired at paths 198 and 199.

Landsat 8 scenes acquired by the paths 198 (up) and 199 (bottom) over the test site. Niclòs et al., 2021.



View of the different land covers at the site: full vegetation cover (left), bare soil (middle) and flooded soil (right). False color composites of L8 OLI (RGB 654). Niclòs et al., 2021.

Methodology: ground measurements

- **Ground TIR radiances were measured along transects** using hand-held Cimel Electronique multiband radiometers model CE-312 (Coll et al., 2019). The surface radiance can be calculated as:

$$L_{\text{surf},i} = \varepsilon_i B_i(T) + (1 - \varepsilon_i) L_{i,a,\text{hem}}^{\downarrow}$$

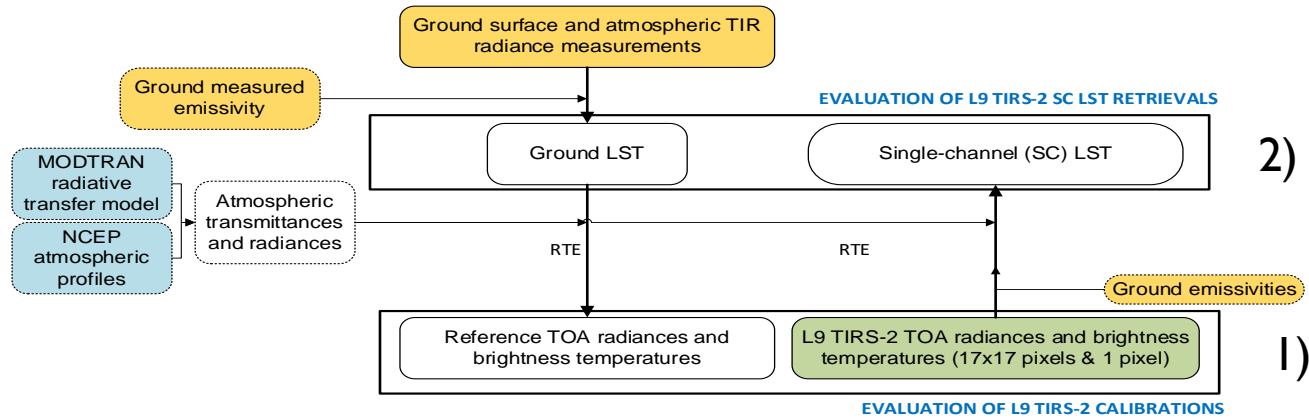
- $L_{\text{surf},i}$ = surface radiance within a spectral band i
- ε_i = surface emissivity
- $B_i(T)$ = channel Planck's function for a temperature T (here T being the LST),
- $L_{i,a,\text{hem}}^{\downarrow}$ = atmospheric downwelling irradiance divided by π , also called downwelling hemispheric radiance (Nicolòs et al., 2018).

- These ground measurements were acquired, **concurrently with L9 overpasses**, for a total of **17 cloud-free days** from December, 2021 to January 2023.

- The radiometers have been recently calibrated in **ESA & CEOS International Thermal Infrared Radiometer Comparison (project FRM4SST) in 2022**.



Methodology



1) **Top-of-atmosphere (TOA) radiances**, L_i , were obtained from ground-measured LSTs with the **radiative transfer equation** (RTE):

$$L_i = \tau_i L_{\text{surf},i} + L_i^{\uparrow a}$$

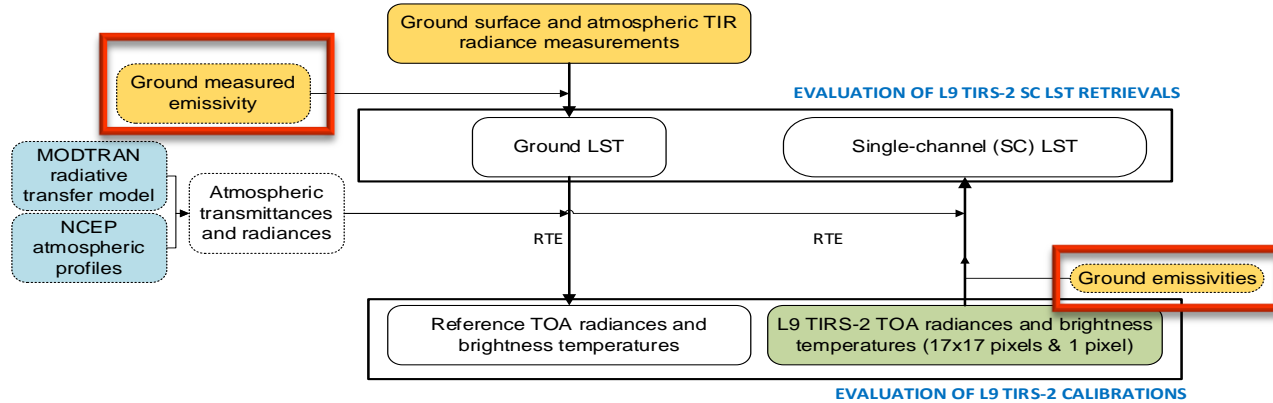
Where τ_i is the atmospheric transmittance and $L_i^{\uparrow a}$ is the upwelling radiance.

2) **A single-channel (SC) correction** is applied to retrieve LSTs from L_i inverting the RTE for $L_{\text{surf},i}$ and then calculate $B_i(T)$.

3) We can also apply **split-window (SW) algorithms** using the both available TIRS-2 bands in Landsat 9.



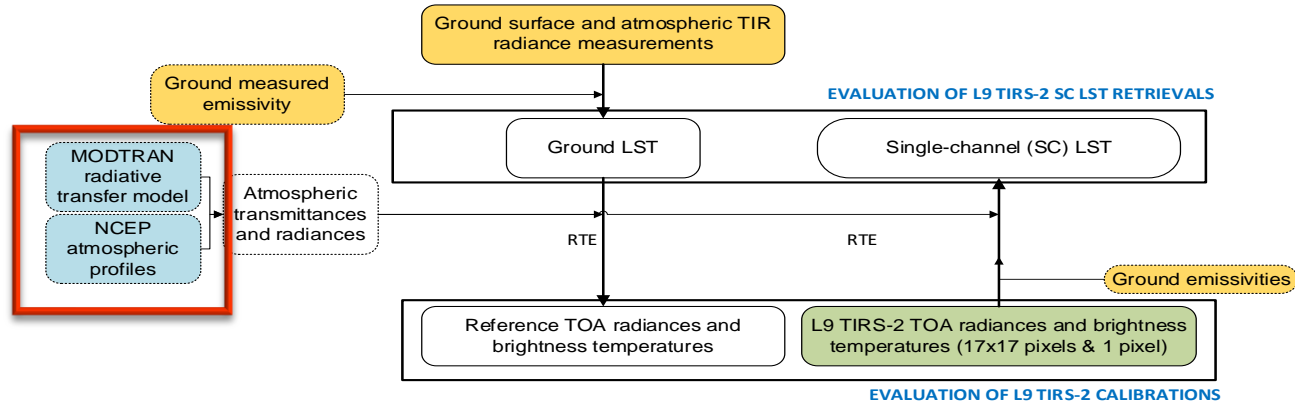
Methodology: land cover emissivities



Emissivity measurements were taken for the different land covers at the site (Nicolòs et al., 2018):

- **Bare soils:** Temperature-Emissivity Separation method (TES).
- **Full vegetation cover:** Box Method.
- **Water surface:** ϵ_i retrieved with L_{surf} equation from radiance measurements and surface temperatures measured by contact probes under controlled conditions.

Methodology: atmospheric simulation

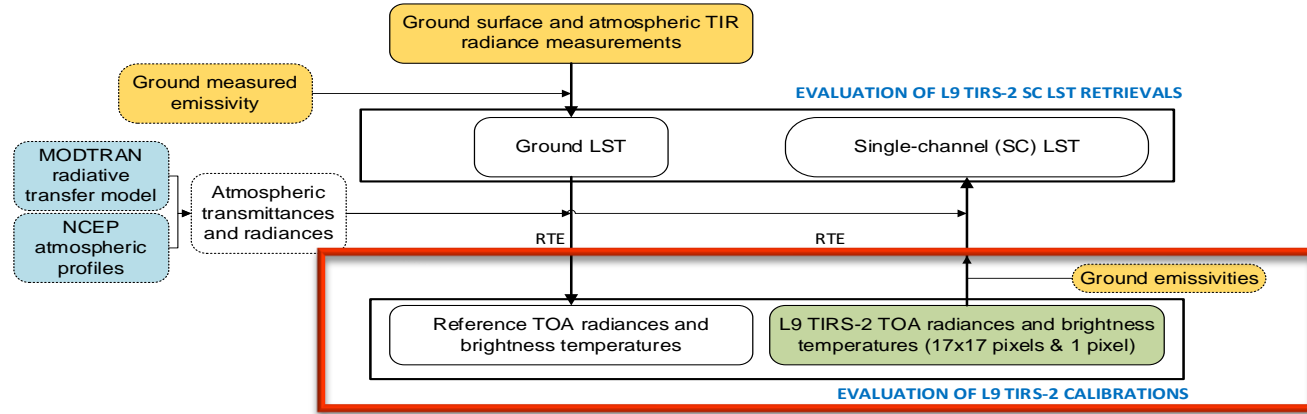


- The atmospheric **transmittance**, τ_i , the **atmospheric downwelling irradiance**, $L_{i,a, \text{hem}}^\downarrow$, and the **upwelling radiance**, $L_{i,a}^\uparrow$, have to be **estimated for each atmospheric condition**.

- Spatial and temporal interpolations of the National Centers for Environmental Prediction (**NCEP**) atmospheric profiles sampled on a $1^\circ \times 1^\circ$ grid and generated every six hours were used as input data to a radiative transfer code, the MODerate resolution atmospheric TRANsmission (**MODTRAN**) 5, **to simulate them**.



Calibration on the Top of Atmosphere (TOA)

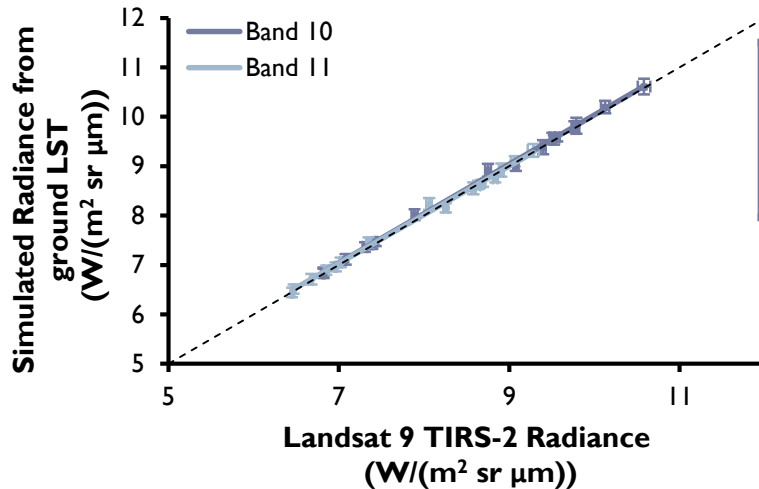


Compare the radiance acquired by Landsat 9 TIRS-2 with the TOA radiance estimated from ground radiance measurements to evaluate the original calibration of the TIRS-2 data



Calibration on the Top of Atmosphere

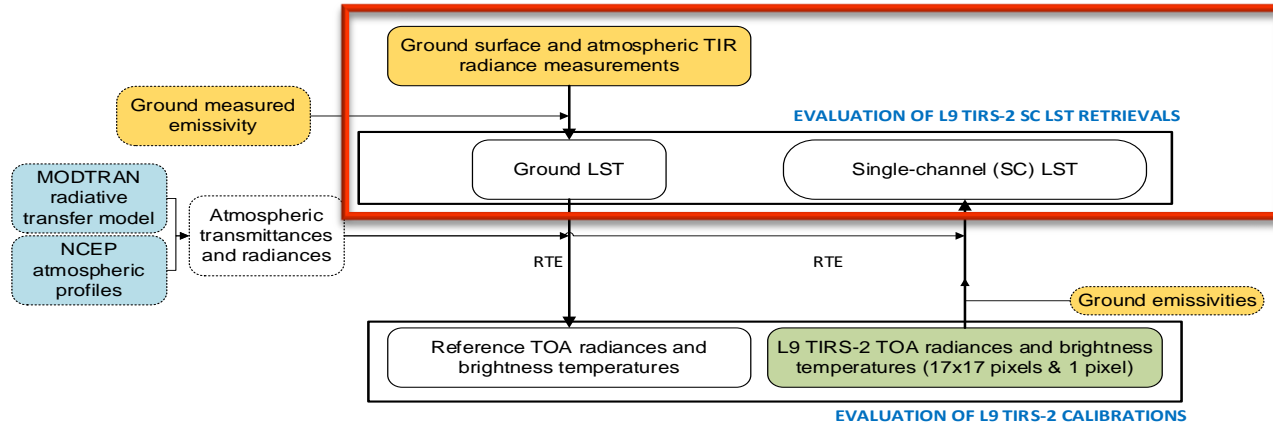
- We use the L9 TIRS-2 LI product which includes two thermal bands, **Band 10** (10.60 to 11.19 μm) and **Band 11** (11.50 to 12.51 μm).
- Statistical results, in terms of **bias (RMSE)** of the difference between L9 TIRS-2 radiance and simulated radiance from ground LST.
- Results are shown for an **array of 17x17 pixels** (resampled to 30m) centered on the test site. This 17x17 is equivalent to 5x5 in the 100m resolution of the TIRS-2 bands.



Band 10		Band 11	
Radiance ($\text{W m}^{-2} \text{sr}^{-1} \mu\text{m}^{-1}$)	Bright. Temp. (K)	Radiance ($\text{W m}^{-2} \text{sr}^{-1} \mu\text{m}^{-1}$)	Bright. Temp. (K)
-0.04 (0.07)	-0.3 (0.5)	-0.01 (0.07)	-0.1 (0.6)

- Both regression coefficient, r^2 , and slope close to 1.
- RMSE around 0.5K in brightness temperature.

Calibration in terms of LST

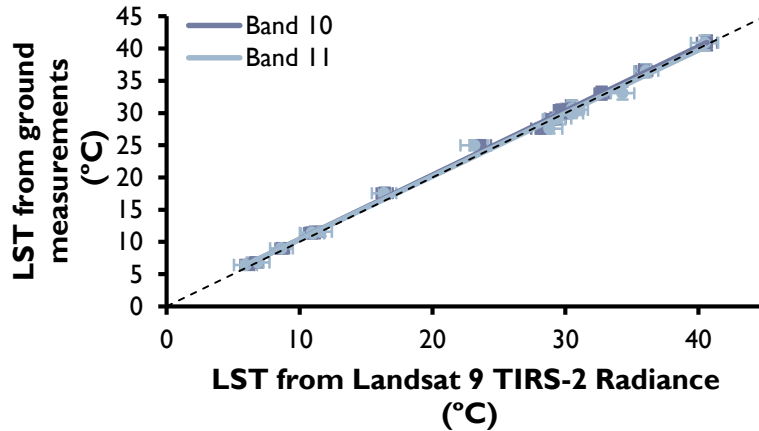


Transform brightness temperatures acquired by L9 into LSTs to be compared with our ground measurements.



Calibration in terms of LST

- We use the L9 TIRS-2 LI product which includes two thermal bands, **Band 10** (10.60 to 11.19 μm) and **Band 11** (11.50 to 12.51 μm).
- Statistical results, in terms of **bias (RMSE)** of the difference between LSTs obtained with a SC correction of TIRS-2 radiances and ground LSTs.
- Results are shown for an **array of 17x17 pixels** (resampled to 30m) centered on the test site.

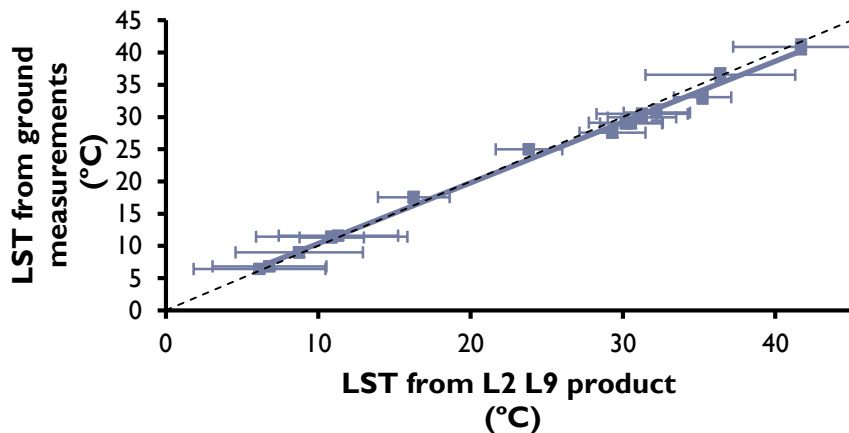


LST B10 (K)	LST B11 (K)
-0.4 (0.6)	-0.1 (0.8)

- Both regression coefficient, r^2 , and slope close to 1.
- RMSE below 1K.

Landsat Collection 2 Level-2 (L2)

- Collection 2 **L2 LST product** is produced using the RTE (SC method) with TIRS-2 band 10, determined from the ASTER Global Emissivity Database (GED), and simulations of atmospheric parameters, performed with the Goddard Earth Observing System Model Version 5 Forward Processing Instrument Teams (GEOS-5-FP-IT) data (Malakar et al., 2018; Meng et al., 2022).
- Statistical results, in terms of **bias (RMSE)** of the difference between LSTs obtained from L2 product and ground LSTs.
- Results are shown for an **array of 17x17 pixels** (resampled to 30m) centered on the test site.



LST L2 (K)
0.4 (1.0)

- Both regression coefficient, r^2 , and slope close to 1.
- RMSE of 1.0 K.

Split-window algorithms

- The L9 sensor has **two TIR bands which allow the use of split-window (SW) algorithms** to obtain LST from atmospheric correction through the differential atmospheric absorption between the two bands.
- We have tested several algorithms from literature:

- 8 parameters, quadratic in T_{10} and T_{11}

$$T = c_0 + \left(c_1 + c_2 \frac{1 - \varepsilon}{\varepsilon} + c_3 \frac{\Delta \varepsilon}{\varepsilon^2} \right) \frac{T_{10} + T_{11}}{2} + \left(c_4 + c_5 \frac{1 - \varepsilon}{\varepsilon} + c_6 \frac{\Delta \varepsilon}{\varepsilon^2} \right) \frac{T_{10} - T_{11}}{2} + c_7 (T_{10} - T_{11})^2$$

- 7 parameters, quadratic in T_{10} and T_{11}

$$T = T_{10} + c_0 + c_1(T_{10} - T_{11}) + c_2(T_{10} - T_{11})^2 + (c_3 + c_4 W)(1 - \varepsilon) + (c_5 + c_6 W)\Delta \varepsilon$$

- 6 parameters, linear in T_{10} and T_{11}

$$T = c_0 + c_1 T_{10} + c_2 (T_{10} - T_{11}) + c_3 \varepsilon + c_4 \varepsilon (T_{10} - T_{11}) + c_5 \Delta \varepsilon$$

Algorithm designed by **Wan & Dozier (1996)** and refined by Wan (2014), fitted for TIRS by Guo et al. (2020) and Gerace et al. (2020).

- Wan, Z., Dozier, J., 1996. A generalized split-window algorithm for retrieving land-surface temperature from space. IEEE Trans. Geosci. Remote Sens. 34, 892–905.
- Guo, J., Ren, H., Zheng, Y., Lu, S., Dong, J., 2020. Evaluation of Land Surface Temperature Retrieval from Landsat 8/TIRS Images before and after Stray Light Correction Using the SURFRAD Dataset. Remote Sens. 12, 1023.
- Gerace, A., Kleynhans, T., Eon, R., Montanaro, M., 2020. Towards an Operational, SplitWindow-Derived Surface Temperature Product for the Thermal Infrared Sensors Onboard Landsat 8 and 9. Remote Sens. 12, 224.

$$B_{10} (T_S) = A_0 L_{10} + A_1 L_{11} + A_2$$

Split-window algorithms

- The L9 sensor has **two TIR bands which allow the use of split-window (SW) algorithms** to obtain LST from atmospheric correction through the differential atmospheric absorption between the two bands.
- We have tested several algorithms from literature:

- 8 parameters, quadratic in T_{10} and T_{11}

$$T = c_0 + \left(c_1 + c_2 \frac{1 - \varepsilon}{\varepsilon} + c_3 \frac{\Delta \varepsilon}{\varepsilon^2} \right) \frac{T_{10} + T_{11}}{2} + \left(c_4 + c_5 \frac{1 - \varepsilon}{\varepsilon} + c_6 \frac{\Delta \varepsilon}{\varepsilon^2} \right) \frac{T_{10} - T_{11}}{2} + c_7 (T_{10} - T_{11})^2$$

Fitted by **Jimenez-Muñoz et al. (2014)**

- Jiménez-Muñoz, J.-C., Sobrino, J.A., Skoković, D., Mattar, C., Cristóbal, J., 2014. Land Surface Temperature Retrieval Methods From Landsat-8 Thermal Infrared Sensor Data. IEEE Geosci. Remote Sens. Lett. 11, 1840–1843.

- 7 parameters, quadratic in T_{10} and T_{11}

$$T = T_{10} + c_0 + c_1(T_{10} - T_{11}) + c_2(T_{10} - T_{11})^2 + (c_3 + c_4 W)(1 - \varepsilon) + (c_5 + c_6 W)\Delta \varepsilon$$

- 4 parameters, linear in T_{10} and T_{11}

$$T = A_0 + A_1 \cdot T_{10} - A_2 \cdot T_{11}$$

$$T = T_{10} + B_1 \cdot (T_{10} - T_{11}) + B_0$$

- 6 parameters, linear in T_{10} and T_{11}

$$T = c_0 + c_1 T_{10} + c_2 (T_{10} - T_{11}) + c_3 \varepsilon + c_4 \varepsilon (T_{10} - T_{11}) + c_5 \Delta \varepsilon$$

- 4 parameters, linear in L_{10} and L_{11}

$$B_{10}(T_S) = A_0 L_{10} + A_1 L_{11} + A_2$$

Split-window algorithms

- The L9 sensor has **two TIR bands which allow the use of split-window (SW) algorithms** to obtain LST from atmospheric correction through the differential atmospheric absorption between the two bands.
- We have tested several algorithms from literature:

- 8 parameters, quadratic in T_{10} and T_{11}

$$T = c_0 + \left(c_1 + c_2 \frac{1 - \varepsilon}{\varepsilon} + c_3 \frac{\Delta \varepsilon}{\varepsilon^2} \right) \frac{T_{10} + T_{11}}{2} + \left(c_4 + c_5 \frac{1 - \varepsilon}{\varepsilon} + c_6 \frac{\Delta \varepsilon}{\varepsilon^2} \right) \frac{T_{10} - T_{11}}{2} + c_7 (T_{10} - T_{11})^2$$

- 7 parameters, quadratic in T_{10} and T_{11}

$$T = T_{10} + c_0 + c_1 (T_{10} - T_{11}) + c_2 (T_{10} - T_{11})^2 + (c_3 + c_4 W)(1 - \varepsilon) + (c_5 + c_6 W) \Delta \varepsilon$$

- 6 parameters, linear in T_{10} and T_{11}

$$T = c_0 + c_1 T_{10} + c_2 (T_{10} - T_{11}) + c_3 \varepsilon + c_4 \varepsilon (T_{10} - T_{11}) + c_5 \Delta \varepsilon$$

Enterprise algorithm fitted by Meng et al. (2020).

Different parameters per W subranges.

- Meng, X., Cheng, J., Zhao, S., Liu, S., Yao, Y., 2019. Estimating Land Surface Temperature from Landsat-8 Data using the NOAA JPSS Enterprise Algorithm. Remote Sens. 11, 155.

- 4 parameters, linear in T_{10} and T_{11}

$$T = A_0 + A_1 \cdot T_{10} - A_2 \cdot T_{11}$$

$$T = T_{10} + B_1 \cdot (T_{10} - T_{11}) + B_0$$

- 4 parameters, linear in L_{10} and L_{11}

$$B_{10} (T_S) = A_0 L_{10} + A_1 L_{11} + A_2$$

Split-window algorithms

- The L9 sensor has **two TIR bands which allow the use of split-window (SW) algorithms** to obtain LST from atmospheric correction through the differential atmospheric absorption between the two bands.

- We have tested several algorithms from literature

- 8 parameters, quadratic in T_{10} and T_{11}

$$T = c_0 + \left(c_1 + c_2 \frac{1 - \varepsilon}{\varepsilon} + c_3 \frac{\Delta \varepsilon}{\varepsilon^2} \right) \frac{T_{10} + T_{11}}{2} + \left(c_4 + c_5 \frac{\Delta \varepsilon}{\varepsilon^2} \right) \frac{T_{10} - T_{11}}{2} + c_6 (T_{10} - T_{11})^2$$

Dependent on emissivities and atmospheric parameters. Top eq. fitted by **Rozenstein** et al. (2014). Bottom eq. Fitted by **Yu** et al. (2014).

- Yu, X., Guo, X., Wu, Z., 2014. Land surface temperature retrieval from Landsat 8 TIRS—Comparison between radiative transfer equation-based method, split window algorithm and single channel method. Remote Sens. 6, 9829–9852.
- Rozenstein, O., Qin, Z., Derimian, Y., Karnieli, A., 2014. Derivation of land surface temperature for Landsat-8 TIRS using a split window algorithm. Sensors. 14, 5768–5780.

- 7 parameters, quadratic in T_{10} and T_{11}

$$T = T_{10} + c_0 + c_1(T_{10} - T_{11}) + c_2(T_{10} - T_{11})^2 + (c_3 + c_4 W)(1 - \varepsilon) + (c_5 + c_6 W)\Delta \varepsilon$$

- 4 parameters, linear in T_{10} and T_{11}

$$T = A_0 + A_1 \cdot T_{10} - A_2 \cdot T_{11}$$

$$T = T_{10} + B_1 \cdot (T_{10} - T_{11}) + B_0$$

- 6 parameters, linear in T_{10} and T_{11}

$$T = c_0 + c_1 T_{10} + c_2 (T_{10} - T_{11}) + c_3 \varepsilon + c_4 \varepsilon (T_{10} - T_{11}) + c_5 \Delta \varepsilon$$

- 4 parameters, linear in L_{10} and L_{11}

$$B_{10} (T_S) = A_0 L_{10} + A_1 L_{11} + A_2$$

Split-window algorithms

- The L9 sensor has **two TIR bands which allow the use of split-window (SW) algorithms** to obtain LST from atmospheric correction through the differential atmospheric absorption between the two bands.
- We have tested several algorithms from literature:

- 8 parameters, quadratic in T_{10} and T_{11}

$$T = c_0 + \left(c_1 + c_2 \frac{1 - \varepsilon}{\varepsilon} + c_3 \frac{\Delta \varepsilon}{\varepsilon^2} \right) \frac{T_{10} + T_{11}}{2} + \left(c_4 + c_5 \frac{1 - \varepsilon}{\varepsilon} + c_6 \frac{\Delta \varepsilon}{\varepsilon^2} \right) \frac{T_{10} - T_{11}}{2} + c_7 (T_{10} - T_{11})^2$$

- 7 parameters, quadratic in T_{10} and T_{11}

$$T = T_{10} + c_0 + c_1 (T_{10} - T_{11}) + c_2 (T_{10} - T_{11})^2 + (c_3 + c_4 W)(1 - \varepsilon) + (c_5 + c_6 W) \Delta \varepsilon$$

- 6 parameters, linear in T_{10} and T_{11}

$$T = c_0 + c_1 T_{10} + c_2 (T_{10} - T_{11}) + c_3 \varepsilon + c_4 \varepsilon (T_{10} - T_{11}) + c_5 \Delta \varepsilon$$

Dependent on emissivities and atmospheric parameters. Fitted by **Wang et al. (2023)**.

- M. Wang et al., "Land Surface Temperature Retrieval From Landsat 9 TIRS-2 Data Using Radiance-Based Split-Window Algorithm," in *IEEE Journal of Selected Topics in Applied Earth Observations and Remote Sensing*, vol. 16, pp. 1100-1112, 2023, doi: 10.1109/JSTARS.2022.3232621.

$$T = A_0 + A_1 \cdot T_{10} - A_2 \cdot T_{11}$$

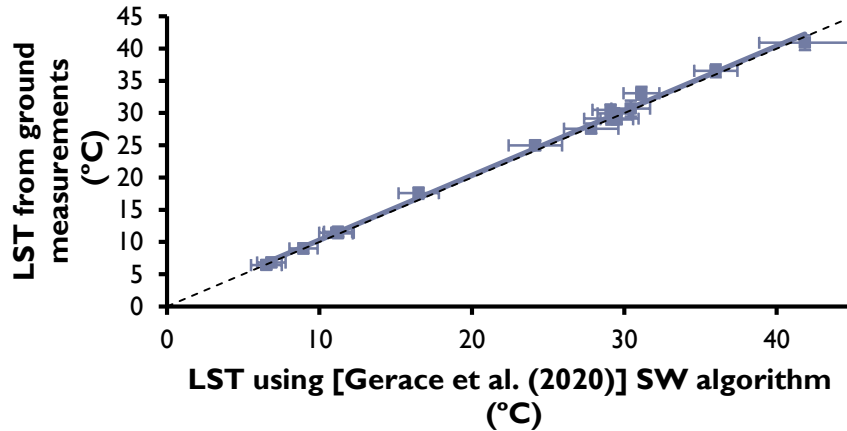
$$T = T_{10} + B_1 \cdot (T_{10} - T_{11}) + B_0$$

- 4 parameters, linear in L_{10} and L_{11}

$$B_{10} (T_S) = A_0 L_{10} + A_1 L_{11} + A_2$$

Split-window algorithms

- The L9 sensor has **two TIR bands which allow the use of split-window (SW) algorithms** to obtain LST from atmospheric correction through the differential atmospheric absorption between the two bands.
- **Gerace et al. (2020)** was proposed as a SW algorithm for a **future operational SW LST product** generated from L8 TIRS and L9 TIRS-2 image data in the Collection 3 processing.



- Both regression coefficient, r^2 , and slope close to 1.

Split-window algorithms

SW algorithm	SW LST – ground LST (K)
Jiménez-Muñoz et al. (2014)	-0.7 (1.0)
Wan and Dozier (1996) by Guo et al. (2020) with coefficients per W and T subranges	0.0 (0.8)
Wan and Dozier by Gerace et al. (2020)	-0.3 (0.8)
NOAA JPSS Enterprise by Meng et al. (2020) per W subranges	-0.3 (0.7)
Yu et al. (2014) with simulated atm. parameters	-0.3 (0.6)
Rozenstein et al. (2014) with simulated atm. parameters	0.1 (0.7)
Wang et al. (2023) with simulated atm. parameters	-0.3 (0.6)
Wang et al. (2023) by calculating atm. parameters in terms of W	-1.3 (1.5)

- Statistical results for the SW algorithms in terms of bias (RMSE).
- Results of the same order than the SC algorithms (for the SW, RMSEs ranged from 0.6 to 1.5 K).

Conclusions

- The original calibration of Landsat 9 TIRS-2 images shows good results at the Valencia Test Site. The RMSD obtained is 0.5 or 0.6 K for bands 10 and 11, respectively, in terms of TOA brightness temperatures.
- SC methods also show good results, both when applying the RTE (RMSD of 0.6 K) and when using the L2 LST product (RMSD of 1.0 K).
- The proposed SW algorithms lead to results of the same order (between 0.6 and 1.5 K). Among them, the SW algorithm proposed by Gerace for Collection 3 is a good option because it provides a negligible systematic uncertainty (0.3 K) and a total uncertainty of 0.8 K at the site.
- The Valencia Test Site has been proven to be a uniform and thermally-homogeneous site with different land covers due to ricepaddy phenology changes, which makes it interesting for CAL/VAL activities under very different surface conditions and temperatures along the year. Both the site and the ground LST acquisition methodology (i.e., along transects within 5 min of each overpass to account for the site variability and the atmospheric turbulence-induced temporal fluctuations) makes the site & procedure promising for the CAL/VAL activities of next missions (LSTM, SBG-TIR, THRSNA, & Landsat-NeXt).

References

- Coll, C., Caselles, V., Galve, J.M., Valor, E., Niclòs, R., Sánchez, J.M., Rivas, R., 2005. Ground measurements for the validation of land surface temperatures derived from AATSR and MODIS data. *Rem. Sens. Environ.* 97, 288–300.
- Coll, C., Caselles, V., Valor, E., Niclòs, R., 2012. Comparison between different sources of atmospheric profiles for land surface temperature retrieval from single channel thermal infrared data. *Rem. Sens. Environ.* 117, 199–210.
- Coll, C., Niclòs, R., Puchades, J., García-Santos, V., Galve, J.M., Pérez-Planells, L., Valor, E., Theocharous, E. (2019) “Laboratory calibration and field measurement of land surface temperature and emissivity using thermal infrared multiband radiometers”, *Int. J. Appl. Earth Obs. Geoinformation*, 78, 227-239.
- Malakar, N., Hulley, G., Hook, S., Laraby, K., Cook, M., Schott, J., 2018. An Operational Land Surface Temperature Product for Landsat Thermal Data: Methodology and Validation. *IEEE Trans. Geosci. Remote Sens.* 2018 (56), 5717–5735.
- Niclòs, R.; Puchades, J.; Coll, C.; Barberà, M.J.; Pérez-Planells, L.; Valiente, J.A.; Sánchez, J.M. Evaluation of Landsat-8 TIRS data recalibrations and land surface temperature split-window algorithms over a homogeneous crop area with different phenological land covers. *ISPRS J. Photogramm. Remote. Sens.* 2021, 174, 237–253, <https://doi.org/10.1016/j.isprsjprs.2021.02.005>.
- Niclòs, R., Pérez-Planells, L., Valiente, J.A., Coll, C., Valor, E., 2018. Evaluation of the SNPP VIIRS Land Surface Temperature product using ground data acquired by an autonomous system at a rice paddy. *ISPRS J. Photogramm. Remote Sens.* 135, 1–12.

ACKNOWLEDGEMENTS

The study was carried out in the framework of the project Tool4Extreme PID2020-118797RBI00 funded by MCIN/AEI/10.13039/501100011033 and the project PROMETEO/2021/016 funded by Generalitat Valenciana.

